Enhanced performance configuration for fast-switching deformed helix ferroelectric liquid crystal continuous tunable Lyot filter

A. M. W. Tam,* G. Qi, A. K. Srivastava, X. Q. Wang, F. Fan, V. G. Chigrinov, and H. S. Kwok

Partner State Key Laboratory on Advanced Displays and Optoelectronics Technologies (PSKL), Department of Electronic and Computer Engineering, Hong Kong University of Science and Technology, Clear Water Bay, Kowloon, Hong Kong, China

*Corresponding author: amwtam@ust.hk

Received 4 March 2014; revised 28 April 2014; accepted 5 May 2014; posted 7 May 2014 (Doc. ID 207468); published 10 June 2014

In this paper, we present a novel design configuration of double DHFLC wave plate continuous tunable Lyot filter, which exhibits a rapid response time of 185 μs, while the high-contrast ratio between the passband and stop band is maintained throughout a wide tunable range. A DHFLC tunable filter with a high-contrast ratio is attractive for realizing high-speed optical processing devices, such as multispectral and hyperspectral imaging systems, real-time remote sensing, field sequential color display, and wavelength demultiplexing in the metro network. In this work, an experimental prototype for a single-stage DHFLC Lyot filter of this design has been fabricated using photoalignment technology. We have demonstrated that the filter has a continuous tunable range of 30 nm for a blue wavelength, 45 nm for a green wavelength, and more than 50 nm for a red wavelength when the applied voltage gradually increases from 0 to 8 V. Within this tunable range, the contrast ratio of the proposed double wave plate configuration is maintained above 20 with small deviation in the transmittance level. Simulation and experimental results showed the proposed double DHFLC wave plate configuration enhances the contrast ratio of the tunable filter and, thus, increases the tunable range of the filter when compared with the Lyot filter using a single DHFLC wave plate. Moreover, we have proposed a polarization insensitive configuration for which the efficiency of the existing prototype can theoretically be doubled by the use of polarization beam splitters.

OCIS codes: (160.3710) Liquid crystals; (130.7408) Wavelength filtering devices; (260.1440) Birefringence; (160.2260) Ferroelectrics.

http://dx.doi.org/10.1364/AO.53.003787

1. Introduction

A switchable birefringence color filter with high efficiency has found numerous important applications in the areas of optical communication [1], spectral imaging [2], remote sensing [3,4], and displays [5]. Liquid crystal tunable filters (LCTF) are employed in most tunable wavelength filtering devices due to their ease of integration in many optical system designs and are capable of displaying high-quality images, low power consumption, and exhibiting a broad range of tunability. Further, no mechanical moving part is required [6].

A Lyot filter is attractive due to its ease of fabrication and simple control required for tuning as compared with other tunable filter technologies such as an acoustic optical tunable filter (AOTF). A Lyot filter can be divided into a series of individual stages. Each stage consists of an LC wave plate sandwiched

1559-128X/14/173787-09$15.00/0

between two parallel or crossed polarizers. The principal axis of the LC wave plate is typically orientated at 45° with respect to the parallel polarizers in order to maximize the tunable spectral range. Wavelength tuning is performed by applying voltage across the LC wave plate, so that the LC director configuration at the wave plate is modified, and hence the effective refractive index is modulated. Moreover, the Lyot filter design requires the retardation of the LC wave plates to be increased by a factor of 2 for each successive stage. Increasing the number of stages of the Lyot filter leads to a finer FWHM bandwidth resolution. The ease of control for the resolution bandwidth through the number of Lyot stages makes Lyot LCTF one of the most popular technologies for many high-resolution tunable devices [7]. To date, the finest FWHM resolution bandwidth that has ever been reported for the Lyot LCTF is 0.1 nm at 532 nm by employing six Lyot stages [8]. This resolution bandwidth is many times finer than a cholesteric tunable filter with a typical bandwidth of 10 nm [9] and AOTF with a typical bandwidth of 1 nm in the visible spectrum at normal incidence [10].

Despite the aforementioned advantages of the Lyot LCTF, most LCTF use a nematic LC in which the tuning response time of the LCTF is typically in the order of tens of milliseconds. This is relatively slow for some applications, such as high-quality field sequential coloring (FSC) display [5,11], hyperspectral imaging for real-time diagnostic in biomedical sensing and imaging [12], and real packet switched wavelength division multiplex access (WDMA) [13], which typically requires a sub-millisecond response time.

More recently, many researches have been devoted to improving the tuning response time of wavelength filtering devices from tens of milliseconds to sub-milliseconds [5,13,14]. One of the possible solutions is to replace the LC from nematic with a ferroelectric liquid crystal (FLC). FLC exhibits spontaneous polarization based on its chiral Smectic C (Sm C*) structure. The response time of the FLC filter is typically in the order of tens to hundreds of microseconds [5,13–15].

Some previous works of the FLC Lyot filter includes operating the FLC wave plate in surface-stabilize FLC (SSFLC) mode [14], for which the FLC helix is suppressed by the anchoring energy of the surface. This not only can achieve rapid tunability (~ sub millisecond) but also has the benefits of high transmission, wide field of view, and large entrance aperture [14]. These advantages make the FLC Lyot filter attractive for the application of hyperspectral imaging, field sequential color display, and wavelength demultiplexing applications. However, the major disadvantage of an SSFLC filter is that continuous wavelength tuning is prohibited, as the wave plate only exhibits two bistable states [14]. Consequently, this imposes a stringent restriction on the flexibility of the system of many optical tunable devices.

The first continuous FLC tunable filter was first realized by Sharp *et al.* [15], employing an Sm A* phase wave plate. However, such a device suffers from the problem of high driving voltage and large degradation in contrast ratio when the filter is electrically tuned. In order to realize a fast response time continuous tunable filter with relatively low driving voltage, one possible solution is to use the FLC wave plate in deformed helix ferroelectric (DHF) mode [5,12]. In fact, Hedge *et al.* [5] has demonstrated that, by simply sandwiching a DHFLC wave plate between a cross or parallel polarizer, a wide continuous tunable range in the visible range can be obtained by either varying the voltage or the driving frequency. However, such simple configuration in [5] suffers from a reduction in transmittance level when the transmittance peak is tuned to another wavelength. The deviation of transmittance level is further enhanced by increasing the number of stages of the Lyot filter. As a result, such simple configuration becomes impractical for some applications such as spectral scanning in hyperspectral imaging, as a large deviation of transmittance is intolerable [16,17]. Another undesirable feature of the configuration proposed in [5] is the trade-off between the increases of the filter resolution bandwidth by increasing the thickness of the plate [see Eq. (8)], which results in an increase in driving voltage ($V = Ed$). As a consequence, the configuration in [5] is only limited to a specific FSC display application and cannot be generalized to other applications at other wavelengths. Subjected to poor contrast ratio in [15] and large deviation in transmittance in [5], this makes the FLC filter difficult to apply into some optical devices.

In this paper, we propose a novel configuration that utilizes a passive phase retarder and two DHFLC cells sandwiched between a pair of parallel polarizers. The helical axes between the DHFLC wave plate are orientated at 45° with respect to the polarization plane. The proposed configuration provides a simple solution for significantly reducing the deviation of transmittance level and enhances the contrast ratio of the filter. These improvements therefore open up a variety of applications for the DHFLC Lyot filter in many tunable optical devices.

2. Theory

As a rule of thumb, the DHF mode appears when the cell gap, d, is roughly 10 times greater than the helix pitch, P_0 [18]. In DHF mode, the helix of the Sm C* material is aligned in a direction governed by the alignment layer of the substrate. The director at each Smectic layer revolves around the cone angle, 2θ, along the azimuth direction at period P_0. In the absence of the electric field, the helical axis (x axis) aligns along the optics axis, as shown in Fig. 1. When an electric field is applied, the polarization, P_S, of the FLC molecules attempts to align in the opposite direction to the applied field. As a result, the FLC directors are reoriented around the cone angle, and hence the FLC helical structure is deformed.

Such deformation, subjected to an applied electric field, leads to a deflection angle, $\Delta\alpha$, between the

helical axis and optics axis as well as changes in effective optical birefringence. Provided the applied electric field, E, is smaller than the critical field of helix unwinding, E_c, given by [19]

$$E_c = \frac{\pi^2}{16}\frac{K_{22}q_0^2}{P_s}, \tag{1}$$

and the frequency of the applied field is smaller than the characteristic angular frequency, ω_c, expressed as [19]

$$\omega_c = \frac{K_{22}q_0^2}{\gamma}, \tag{2}$$

the average deflection angle, $\langle\alpha\rangle$, and the effective birefringence, $\langle\Delta n_{\text{eff}}\rangle$, reads [19]

$$\langle\alpha(E)\rangle = \frac{\sin 2\theta\pi^2 E}{64(1-3/2\sin^2\theta)E_c}, \tag{3}$$

$$\langle\Delta n_{\text{eff}}(E)\rangle = \Delta n\left(1+\frac{\sin^2 2\theta}{1-3/2\sin^2\theta}\left(\frac{\pi^2}{32E_c}\right)^2 E^2\right), \tag{4}$$

where γ is the rotational viscosity of the FLC, $\Delta n = n_e - n_o$ is the optical birefringence in the absence of E field, and θ is the tilt angle of the FLC material. The electro-optical properties of the FLC wave plate is described by Eqs. (3) and (4) in which the mean angle deviation $\langle\alpha\rangle$ of the planar FLC wave plate is linearly related to the applied E field, while the average electrically induced birefringence $\langle\Delta n_{\text{eff}}\rangle$ is related to the square of the applied E field. This is different from the nematic LC wave plate, where the electrically induced birefringence is linearly proportional to the E field, and the optics axis does not deviate with respect to the applied E field [20].

Once $\langle\alpha(E)\rangle$ and $\langle\Delta n_{\text{eff}}(E)\rangle$ are determined, the output transmittance of a DHFLC wave plate sandwiched between two parallel polarizers in Fig. 1 can therefore be computed using the relation [5,18]

$$T = \frac{1}{2}\left[1-\sin^2[2(\beta-\langle\alpha(E)\rangle)]\sin^2\left(\frac{\pi d\langle\Delta n_{\text{eff}}(E)\rangle}{\lambda}\right)\right], \tag{5}$$

where λ is the wavelength of the optical input. A factor of ½ is present, as 50% of the light is absorbed by the first polarizer. From Eq. (5), local maxima of the passband is determined to be

$$\lambda_{\max} = \frac{\langle\Delta n_{\text{eff}}(E)\rangle d}{m}, \tag{6}$$

where m is a positive integer. Equation (6) implies that, by controlling the retardation parameter $\Delta n_{\text{eff}}d$ via the E field, continuous tunable optical filtering can be designed where the wavelength transmittance peak is modified with respect to the strength of the E field. Using Eq. (6), the free spectral range (FSR) of the FLC optical filter is therefore given by

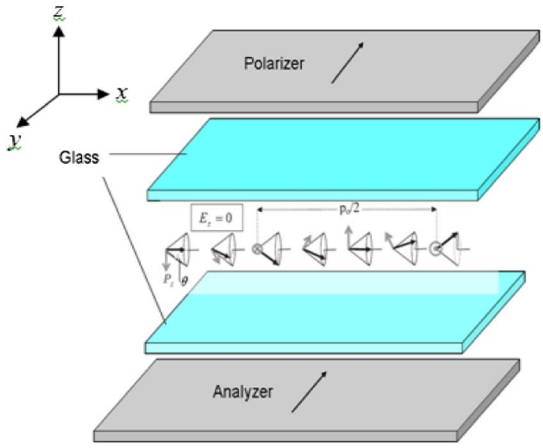

Fig. 1. Structure of DHFLC wave plate with FLC director spatially rotated in the azimuth direction at period P_0.

$$\text{FSR} = \Delta\lambda = \frac{\lambda^2}{\langle\Delta n_{\text{eff}}(E)\rangle d}. \tag{7}$$

The bandwidth of the tunable Lyot filter can be controlled by cascading several individual Lyot stages. The FWHM bandwidth of an N stage Lyot filter can be approximated as [7]

$$\Delta\lambda_{1/2} = \frac{0.886\lambda^2}{2^N\langle\Delta n_{\text{eff}}(E)\rangle d}. \tag{8}$$

The filter bandwidth can therefore be reduced exponentially by increasing N. Note that increasing the number of Lyot stages does not change the FSR of the optical filter.

Provided $E \ll E_c$, the switching response time of the FLC filter can be theoretically determined using the relation [5,18],

$$\tau = \frac{\gamma}{K_{22}q_0^2}, \tag{9}$$

Equation (9) shows that the response time of the optical filter is cell gap independent and is rapid provided the FLC material has a short helix pitch (large q_0). Response times in the order of 100 μs have been reported for the DHFLC wave plate with a helix pitch less than 1 μm [21].

3. Design Methodology

Although wavelength tuning can be achieved from the structure proposed in Fig. 1, Eq. (5) reveals the transmittance at the rejection band increases with respect to the applied electric field due to the deviation of optics axis $\alpha(E)$. This is highly undesirable for many applications where a significant portion of an unwanted signal will be transmitted to the receiver, which will distort and obscure the signal within the spectral region of interest.

For a standard Lyot filter, the bandwidth can typically be controlled by adding a passive phase retarder prior to LC wave plates [22], as shown in Fig. 2(a). This configuration effectively reduces the correlation between the bandwidth and the operating

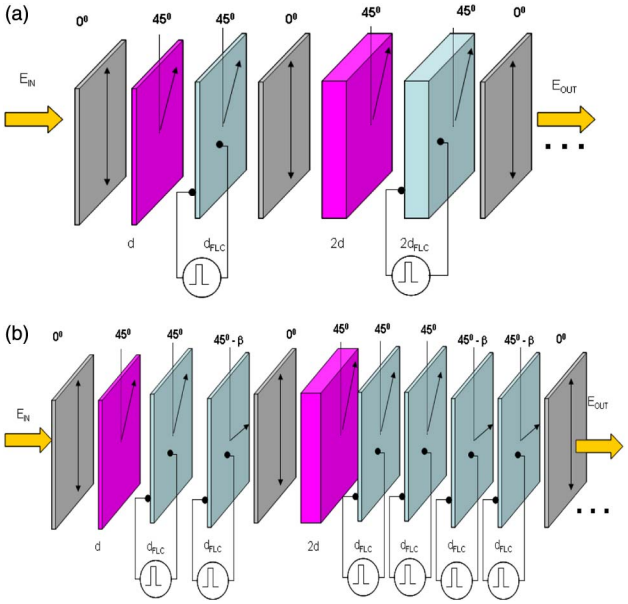

Fig. 2. Continuous tunable DHFLC Lyot filter configuration with passive retarder and DHFLC retarder sandwiched between two parallel polarizers. (a) Typical single DHFLC configuration. (b) Proposed double DHFLC wave plate configuration.

voltage; thus a desirable operating voltage can be maintained simultaneously. However, we have discovered that, when subjected to the deflection of optics axis from the applied E field $\langle\alpha(E)\rangle$, a property that is inherent in the electro-optics of DHFLC, leads to a high transmittance level at the rejection band [see Figs. 3(a) and 4(a)]. Therefore we can conclude that such conventional configuration used in the nematic LC filter is inappropriate for the DHFLC filter.

In this paper, we have developed a configuration that resolves the existing problems of a DHFLC filter such as significantly reducing the variation between the maximum transmittance levels subjected to an applied E field. In addition, good control over the operating voltage and bandwidth is maintained, with high transmittance at the passband and low transmittance at the rejection band. Our modified configuration of a single Lyot stage is shown in Fig. 2(b), which involves a passive phase retarder that is orientated at an angle of 45° with respect to the polarizer to control the filter bandwidth and two electrically tunable DHFLC wave plates. The helical axis of the first DHFLC wave plate is aligned with the optics axis of the passive phase retarder in the absence of applied voltage, while the other DHFLC wave plate, which is identical to the first wave plate, is orientated at an angle, β, with respect to the first DHFLC wave plate in the plane of polarization. Both wave plates are applied from the same electric signal.

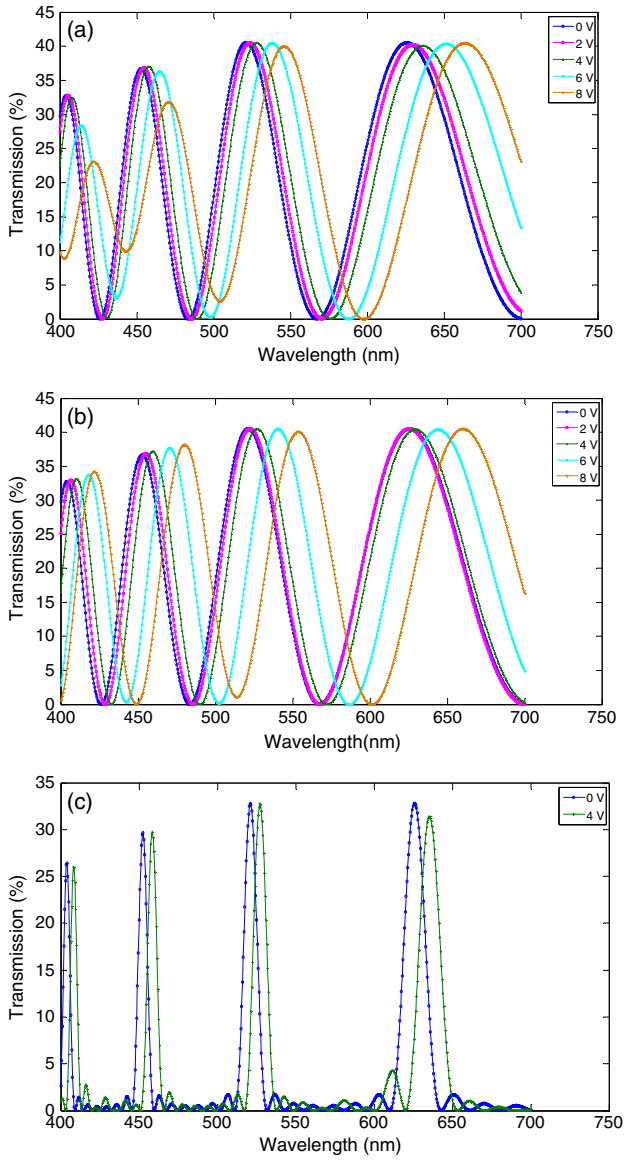

Fig. 3. Simulation results of transmission spectrums for (a) single DHFLC wave plate single-stage Lyot filter, (b) double DHFLC wave plate single-stage Lyot filter, and (c) three-stage double wave plate DHFLC Lyot filter.

In the theoretical calculation, the incident light denoted by $\mathbf{E_{in}}$ is unpolarized and can be expressed as $E_{\in} = (E_0/\sqrt{2})[^1_1]$. The output transmittance is determined after passing through the analyzer (2nd polarizer), phase retarder with retardation Γ_p, the DHFLC wave plates with electrically dependent retardation $\Gamma(E)$, the output transmittance T_{out} can be computed using the Jones matrix approach [23]:

$$T_{\text{out}} = \left|\frac{E_{\text{out}}}{E_{\text{in}}}\right|^2 = \frac{|PR(a)G(\Gamma)R(-a)R(b)G(\Gamma)R(-b)R(45°)G(\Gamma_p)R(-45°)PE_{\text{in}}|^2}{E_0^2}$$
$$= \frac{1}{2}\left(|X|^2\cos\left(\frac{\Gamma_p}{2}\right) + |Y|^2\sin^2\left(\frac{\Gamma_p}{2}\right) - \text{Im}(XY^*)\sin\Gamma_p\right), \quad (10)$$

where $X = \cos^2\beta\cos\langle\Gamma(E)\rangle + \sin^2\beta - i\cos(90° + 2\langle\alpha(E)\rangle - \beta)\sin\langle\Gamma(E)\rangle$, $Y = \cos\beta[\sin\beta\cos\langle\Gamma(E)\rangle - i\sin(90° + 2\langle\alpha(E)\rangle - \beta)\sin\langle\Gamma(E)\rangle] + 1/2\sin 2\beta$, $R(\psi) = \begin{pmatrix}\cos\psi & -\sin\psi \\ \sin\psi & \cos\psi\end{pmatrix}$ is the rotational matrix, $P = \begin{pmatrix}1 & 0 \\ 0 & 0\end{pmatrix}$ is the transmission matrix of the polarizer with the transmission axis aligned in the x direction, $G(\delta) = \begin{pmatrix}e^{\frac{-i\delta}{2}} & 0 \\ 0 & e^{\frac{i\delta}{2}}\end{pmatrix}$ is the matrix for phase retarder, $\langle\Gamma(E)\rangle = (2\pi\langle\Delta n_{\text{eff}}(E)\rangle d_1/\lambda)$ is the phase retardation of the electrically tunable DHFLC wave plates with thickness d_1, $\Gamma_p = (2\pi\Delta n d_2/\lambda)$ is the phase retardation of the passive phase retarder with thickness d_2, and β is the azimuth angle difference between the optics axis of the FLC wave plates.

Because the transmittance T_{out} is dependent on the angle difference between the FLC wave plates, β, the objective of this design is therefore to optimize the angle, β, such that the transmittance in the passband is sufficiently large while the contrast between the passband and the rejection band is maximized in the spectral region of interest ($\lambda = 500$ to 700 nm) for a sufficient range of applied field, i.e., $E < 0.3E_c$. Consequently, we introduce the optimization function Q as follows:

$$\max[Q_E(\beta)] = \frac{\sum_{k=1}^{L}[I_k^{\max}(\beta)]^2}{\sum_{k=1}^{M}[I_k^{\min}(\beta)]^2}, \tag{11}$$

where $I_k^{\max}(\beta)$ and $I_k^{\min}(\beta)$ represent the transmittance of the kth maxima and minima of the corresponding spectral region of interest, respectively. Although the expression of T_{out} indicates $Q_E(\beta)$ approach ∞ when β is 90° irrespective to the applied E field, this condition must be discarded. This is because, in the case of 90°, the transmittance would be independent of $\Gamma(E)$, which therefore signifies the filter cannot be electrically tuned. As a result, the optimum angle β is scanned between the ranges 0°–85° to ensure the optimization function of Q is satisfied while the maxima of T_{out} can be electrically modulated.

For a small applied field, i.e., $E < 0.5E_c$, the optimum angle turns out to be insensitive to the applied field where it typically falls within the narrow range of 43°–46°. This is an important result that we have discovered, as this implies there is an electrical tunable range that can be used for resolving the aforementioned problems, i.e., contrast ratio, deviation of optics axis etc. of the DHFLC filter by simply orientating the second DHFLC wave plate at an angle of ~45° in the polarization plane with respect to the first one. Numerical simulation shows this electrical tunable range is broadened for FLC materials with shorter P_0.

4. Experimental Procedure

In this work, photoalignment technology is used so that good and stable alignment of FLC molecules is achieved without physical contact, which therefore minimizes the number of defects. Moreover, the anchoring energy can be regulated using photoalignment by simply controlling the exposure time of the UV irradiation, which is crucial to obtain good alignment for FLC materials.

Sulfonic azo-dye SD-1 is used as the photoalignment material. Before depositing SD-1 onto the substrate of the wave plate, the SD-1 is dissolved in N, N dimethylformamide (DMF) at a concentration of 0.5 w/w%. The solution is spin coated onto the ultraviolet-ozone (UVO) treated ITO glasses, which is used as the substrate of the wave plate, at 3000 rpm for 30 s, and then baked at 100°C for 10 min to remove excess DMF on the substrate. After these processes, a thin molecular photoaligning layer of SD-1 is prepared onto the substrate.

The alignment orientation of the SD-1 layer is controlled by irradiating linear polarized UV light at a wavelength of 365 nm. When UV light is absorbed by the azo-dye molecules, the chromophore of the molecules tends to rotate perpendicularly in the azimuth direction with respect to the direction of polarization of the UV light [24]. With a light intensity of 3 mW/cm^2 at 320 nm wavelength, the exposure time required is 120 min to give good planar alignment.

One of the photoaligned ITO glass substrate is then deposited with 4 μm calibrated spacers, which corresponds to the thickness of the wave plate, and, subsequently, two glass plates are assembled using epoxy glue. The assembled wave plate is then infiltrated with FLC-576, developed by P.N. Lebedev Physical Institute of Russian Academy of Sciences, with an optical birefringence of $\Delta n = 0.19$, a helix pitch of $P_0 = 200$ nm, a tilt angle of $\theta = 32°$, and a spontaneous polarization of $P_s = 130$ nC/cm^2 at room temperature. The infiltration of FLC is performed under capillary action, and the process is conducted inside a vacuum chamber at temperature 3°C above clearing point (113°C). FLC-576 is used in this work because the helix pitch is short, which is ideal for increasing the desired tunable range of the filter.

5. Results and Discussions

A. Simulation Results

In this work, an optical filter is designed in which the transmission peaks are located at 450 nm in the blue region, 520 nm in the green region, and 620 nm in the red region in the absence of applied voltage. A phase retarder with retardation $\Delta nd = 1800$ nm at 550 nm, and 4 μm FLC-576 wave plates are selected to satisfy this condition. The helical axis between the DHFLC wave plates is offset at an angle 45°, i.e., $\beta = 45°$. Simulation results for the transmittance spectrum for a single-stage Lyot filter using a single FLC wave plate [see Fig. 2(a)] is shown in Fig. 3(a), while the simulated transmittance for a single-stage Lyot filter using a double FLC wave plate configuration [see Fig. 2(b)] is shown in Fig. 3(b). By comparing the troughs of Figs. 3(a) and 3(b), we can identify that

the double FLC wave plate configuration drastically reduces the transmittance at the rejection band subjected to an increase in the electric field. Moreover, Fig. 3(b) shows the double FLC wave plate configuration has much smaller deviation for the transmittance level at the passband when compared with the single FLC wave plate configuration. As a result, we can conclude the double FLC configuration significantly improves the contrast ratio between the passband and rejection band. This improvement can be understood by the change in phase retardation due to the deviation of optics axis from the first DHFLC wave plate being compensated by the second DHFLC wave plate with the optic axis deviated by the same amount when both wave plates are controlled by the same voltage signal. It should be noted that the contrast improvement of the proposed double DHFLC configuration is not limited to the visible range at 400–700 nm, where this holds also for wavelengths in the infrared region, i.e., at 1500 nm. The transmittance peak is limited at 40% in Figs. 3(a) and 3(b) because we have assumed the polarizer has a maximum transmittance of 90% at its transmission axis. The reduction in transmission level in the passband below 500 nm is a consequence of a visible dichroic polarizer, which typically has greater absorption for those wavelengths.

Equation (8) implies that the filter bandwidth can be reduced further by introducing more filtering stages. Simulation results in Fig. 3(c) show that, for a three-stage double wave plate DHFLC Lyot filter, the FWHM bandwidth is narrowed to less than 15 nm for transmission peaks in the visible region. When a 4 V voltage signal is applied to the filter, Fig. 3(c) shows the transmission peak shifts from 525 to 535 nm, where the amount of shift is similar to that in Fig. 3(b). Results in Fig. 3(c) also show good suppression in the rejection band using the proposed configuration with small deviation in transmittance level at the passband when the filter is tuned from 0 to 4 V. However, by introducing more Lyot stages, the peak transmittance is reduced to less than 35% as more wave plates and polarizers are added into the system, which increases the absorption and reflection losses of the filter.

B. Experimental Results

In order to verify the theoretical simulation of Figs. 3(a) and 3(b), an experimental prototype for a single-stage DHFLC Lyot filter for a single and double FLC wave plate configuration has been fabricated using photoalignment technology. A single-stage Lyot filter is sufficient enough to demonstrate the advantages of the proposed double FLC wave plate configuration, i.e., contrast ratio enhancement, small deviation in transmission peaks during tuning etc. This is because from Eqs. (6) and (7), the FSR, the range of tunability, and the transmission peaks and troughs of the tunable filter are all governed by the thickness of FLC wave plates at the first stage of the filter.

The properties of the prototype are tested and measured by the CG 100 optical spectrum analyzer system. The measurement system consists of a white light source that illuminates the filter located at the testing bench. The polarizer and analyzer of the polarization microscope is configured in the same direction. The fiber optics spectrometer measures the transmission spectrum of the filter, and the measured data from the spectrometer will then be sent to the computer via a fiber optics cable to process and display the measured spectrum.

The experimentally measured transmittance spectra for a single FLC and double FLC wave plate for different applied voltages are shown in Figs. 4(a) and 4(b), respectively. Comparison between Figs. 3(a) and 3(b) and Figs. 4(a) and 4(b) shows that the simulation and experimental results of the transmission peaks and troughs are generally in good agreement throughout the visible spectrum for the corresponding applied voltages. Both simulation [Figs. 3(a) and 3(b)] and experimental results reveal [Figs. 4(a) and 4(b)] that the contrast ratio of the proposed double FLC wave plate configuration is enhanced as compared with the single FLC wave plate configuration when the voltage increase from 0 to 8 V. Additionally, subjected to a continuous increase in applied voltage, experimental results in Figs. 4(a) and 4(b) show that the transmission peak shifts continuously. Figure 4(b) shows the transmission peak in the blue region shifts roughly by 30 nm from 450 to 480 nm; while in the green region, the transmission peak shifts by 45 nm from 520 to 565 nm; and in the red region, the transmission peak shifts by more than 50 nm from 620 to beyond 673 nm. Figure 4(b) also shows that the transmittance level of the passband has a deviation of less than 4% when the voltage is applied within 0 to 8 V.

A direct comparison between the simulation and experimental result for the double wave plate configuration is shown in Fig. 4(c). Comparisons between Figs. 3(b) and 4(b), as well as Fig. 4(c), show that the transmittance of the experimental results is about 10% smaller than simulation results due to the diffraction and scattering loss of the DHFLC wave plate. Moreover, experimental results show this mismatch in transmittance at the passband gradually increases for wavelengths below 500 nm. This can be explained by the absorption of the SD-1 alignment layer, which becomes more significant for wavelengths below 500 nm [24].

Since the visible range considered (400–700 nm) consists of a multiple number of maxima and minima, the contrast ratio of the transmission band and rejection band of the DHFLC tunable filter is defined to be

$$CR(V) = \frac{\sum_{k=1}^{M} I_k^{\max}(V)/M}{\sum_{k=1}^{L} I_k^{\min}(V)/L}, \tag{12}$$

where $I_k^{\max}(V)$ and $I_k^{\min}(V)$ is the kth transmission maxima and minima of the filter in the spectral

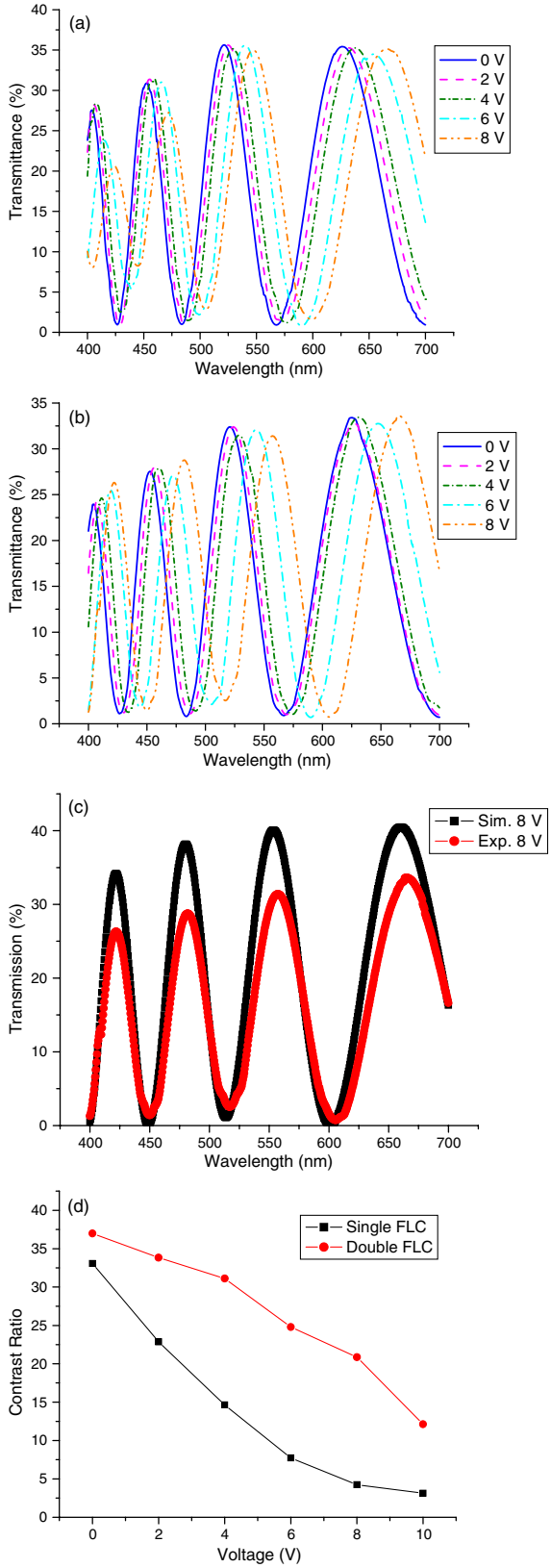

Fig. 4. Experimental measurement of single-stage DHFLC filter. (a) Transmittance for single DHFLC configuration. (b) Transmittance for double DHFLC configuration. (c) Direct comparison between simulation result and experimental result for 8 V applied voltage. (d) Contrast ratio against applied voltage for single and double FLC wave plate configuration.

range of interest (400–700 nm) for different applied voltage; M and L is the number of maxima and minima within the visible range of the spectrum. A plot of the contrast ratio defined in Eq. (12) against applied voltage of the DHFLC filter prototype for a single FLC and double FLC wave plate configuration is shown in Fig. 4(d). For voltages that are within 0–8 V, the contrast ratio of the double FLC wave plate configuration is maintained above 20, while the contrast ratio sharply decreases below 10 for a single FLC wave plate configuration. However, for voltage levels that exceed 8 V, the contrast ratio for a double FLC wave plate configuration also decreases below 20 because the effect of deviation in optics axis is large enough to have a significant impact on the contrast ratio of the double wave plate configuration.

The response time of the filter is governed by the switching time of the FLC wave plate. The switching time of the 4 μm FLC wave plate is determined by sandwiching the FLC wave plate between two cross polarizers, as shown in Fig. 5(a). The FLC wave plate is driven by 500 Hz rectangular pulse AC voltage [as shown in Fig. 5(b)]. The transmittance level of the system detected by the photodiode is shown in Fig. 5(b). When no voltage is 0 V, the transmittance level approaches 0, as the optics axis of the FLC wave plate is aligned along the polarizer. However, once the voltage is applied, the optics axis of the FLC wave plate deviates, and hence a portion of the incident light is detected by the photodiode. The switching time (filter response time) is determined by adding the 10%–90% rise and fall time from the transmittance curve. Throughout the voltage range of 2–8 V, which is small in comparison with the unwinding voltage (~18 V for a 4 μm thick FLC-576 wave plate), our measurement shows the filter exhibits a fast response time of ~185 μs, which agrees with the results presented in [21].

C. Polarization Independent DHFLC Filter

The transmittance of a DHFLC Lyot filter can be improved by using the polarization beam splitter (PBS) configuration shown in Fig. 6. In this configuration, the filter is polarization insensitive for which the optical power of both polarization components of the incoming optical signal is being utilized. In this configuration, the two linear polarizations, which are orthogonal to one another, are divided into two independent paths by the PBS 1. A double wave plate DHFLC filter will be added in each of the paths for optical filtering. The configuration of DHFLC filter A and filter B in Fig. 6 almost has the same configuration, but polarizers of filter A are parallel to the x axis while the polarizers in filter B are parallel to the y axis. The filtered signal of both independent polarization components at each different path will be recombined at PBS 2; thus the efficiency can theoretically be doubled for the configuration in Fig. 6. However, the size of the filter is expected to increase several times at the expense of improving the optical throughput of the filter in this design.

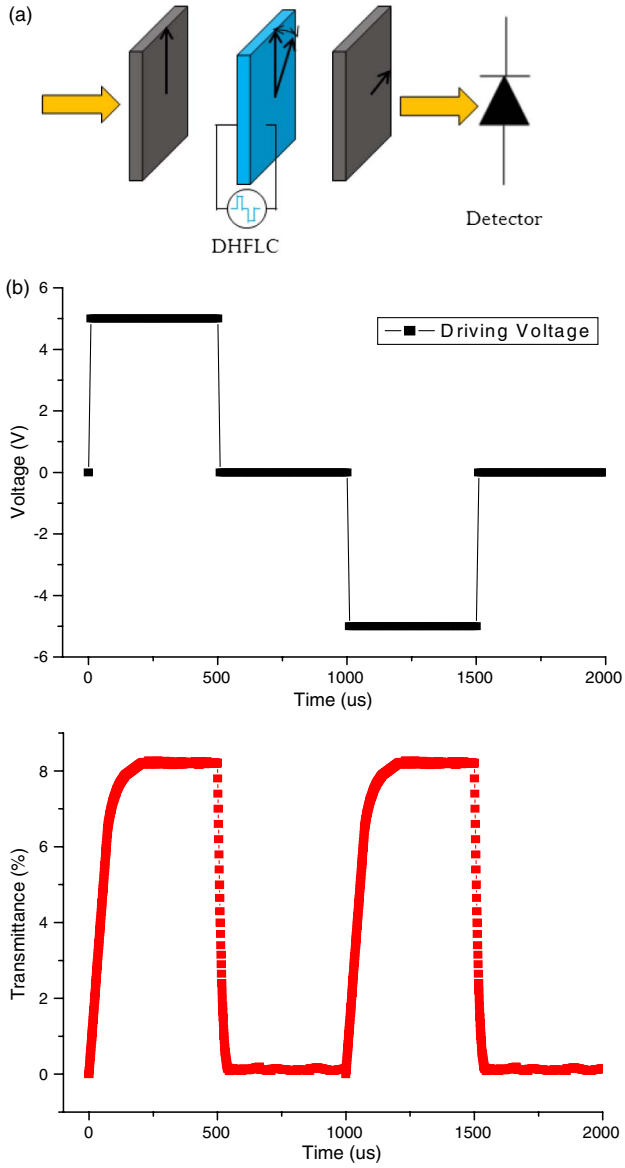

Fig. 5. Experimental measurements of DHFLC filter response time. (a) Measurement setup of DHFLC response time. (b) 4 μm DHFLC wave plate response with respect to ±5 V AC square-wave voltage signal.

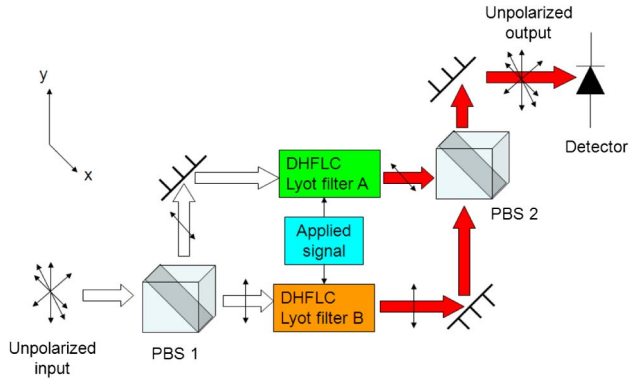

Fig. 6. Increase in output intensity using PBS to design a polarization independent DHFLC tunable filter.

6. Conclusions

In conclusion, the contrast ratio and the deviation of transmittance of a compact, fast-switching continuous tunable DHFLC Lyot filter is substantially enhanced by our simple proposed configuration via the use of two DHFLC wave plates with a 45° angle offset between their optics axis in the plane of polarization. We believe that this simple advancement of the DHFLC Lyot filter can potentially be applied to improve the performance of many existing fast-response-time electro-optical devices; for example, FSC, illumination control in optical microscopy, real-time hyperspectral imaging sensor for biomedical sensing and imaging. Moreover, a polarization insensitive DHFLC tunable Lyot filter has been proposed, which can theoretically double the efficiency of a polarization sensitive filter by the use of PBS, but at the expense of increasing the size of the filter several times.

The HKUST grant ITP/039/12NP is gratefully acknowledged for supporting this work.

References

1. Z. Luo and Z. Wan, "Design and tolerance analysis of optical interleaver based on retardant crystals," Opt. Int. J. Light Electron Opt. **122**, 133–135 (2011).
2. N. Tsumura, H. Sato, T. Hasegawa, H. Haneishi, and Y. Miyake, "Limitation of color samples for spectral estimation from sensor responses in fine art painting," Opt. Rev. **6**, 57–61 (1999).
3. G. A. Kopp, M. J. Derks, D. M. Hassler, J. C. Woods, J. L. Streete, and J. G. Blankner, "Tunable liquid-crystal filter for solar imaging at the He I 1083 nm line," Appl. Opt. **36**, 291–296 (1997).
4. B. N. Rock, J. E. Vogelmann, D. L. Williams, A. F. Vogelmann, and T. Hoshizaki, "Remote detection of forest damage," Bioscience **36**, 439–445 (1986).
5. G. Hedge, P. Xu, E. Pozhidaev, V. Chigrinov, and H. S. Kwok, "Electrically controlled birefringence colours in deformed helix ferroelectric liquid crystals," Liq. Cryst. **35**, 1137–1144 (2008).
6. H. Morris, C. Hoyt, and P. Treado, "Acousto-optic and liquid crystal tunable filters," Appl. Spectrosc. **48**, 857–866 (1994).
7. P. Yeh, "Dispersive birefringent filters," Opt. Commun. **37**, 153–158 (1981).
8. J. Staromlynska, S. M. Rees, and M. P. Gillyon, "High performance tunable filter," Appl. Opt. **37**, 1081–1088 (1998).
9. Y. Wong, Q. Sun, and H. Zhang, "Widely tunable optical filter with variable bandwidth based on spatially distributed cholesteric liquid crystal," Opt. Eng. **52**, 044003 (2013).
10. Acousto Optic Tunable Filters Application Notes (ISOMET 1998), Chap. 3.
11. P. Bos, T. Buzak, and R. Vatne, "A full-color field-sequential color display," Proc. Soc. Inf. Disp. **26**, 157–161 (1985).
12. S. J. Woltman, G. D. Jay, and G. P. Crawford, "Liquid crystal materials find a new order in biomedical applications," Nat. Mater. **6**, 929–938 (2007).
13. A. Sneh and K. M. Johnson, "High speed continuously tunable liquid crystal filter for WDM networks," J. Lightwave Technol. **14**, 1067–1080 (1996).
14. H. J. Masterson, G. D. Sharp, and K. M. Johnson, "Ferroelectric liquid-crystal tunable filter," Opt. Lett. **14**, 1249–1251 (1989).
15. G. D. Sharp, K. M. Johnson, and D. Doroski, "Continuously tunable smectic A* liquid-crystal color filter," Opt. Lett. **15**, 523–525 (1990).
16. T. Vo-dinh, D. Stokes, M. Wabuyele, M. Martin, J. Song, R. Jagannathan, E. Michuad, R. Lee, and X. Pan, "A hyperspectral imaging system for in vivo optical diagnostics. Hyperspectral imaging basic principles, instrumental systems, and

applications of biomedical interest," IEEE Eng. Med. Biol. Mag. **23**, 40–49 (2004).
17. B. Peterson, *Spectrum Analysis Basics Application Note 150* (Agilent Technologies, 2013).
18. V. G. Chigrinov, *Liquid Crystal Devices—Physics and Applications* (Artech House, 1999).
19. E. Pozhidaev, S. Torgova, M. Minchenko, C. A. R. Yednak, A. Strigazzi, and E. Miraldi, "Phase modulation and ellipticity of the light transmitted through a smectic C* layer with short helix pitch," Liq. Cryst. **37**, 1067–1081 (2010).
20. D. Yang and S. Wu, *Fundamentals of Liquid Crystal Devices*, Wiley-SID Series in Display Technology (Wiley, 2006).
21. Q. Guo, Z. Brodzeli, E. P. Pozhidaev, F. Fan, V. G. Chigrinov, H. S. Kwok, L. Silvestri, and F. Ladouceur, "Fast electro-optical mode in photo-aligned reflective deformed helix ferroelectric liquid crystal cells," Opt. Lett. **37**, 2343–2345 (2012).
22. G. Kopp, "Tunable birefrigent filters using liquid crystal variable retarders," Proc. SPIE **2265**, 193–201 (1994).
23. R. C. Jones, "A new calculus for the treatment of optical systems, III the Sohncke theory of optical activity," J. Opt. Soc. Am. **31**, 500–503 (1941).
24. V. G. Chigrinov, V. M. Kozenkov, and H. S. Kwok, *Photoalignment Liquid Crystalline Materials, Physics and Applications* (Wiley, 2008).